Journal of Thermal Engineering
Web page info: https://jten.yildiz.edu.tr
DOI: 10.14744/thermal.0000985

Journal of Thermal Engineering

Research Article

Comparative performance analysis of the Andasol-1 power plant in M'sila (an Algerian province)

Khaled BOUCHAREB[1,2], Nabila IHADDADENE[1,3,*], Razika IHADDADENE[1,3], Khellaf BELKHIRI[1]

[1]*Department of Mechanical Engineering, M'Sila University, M'Sila, 28000, Algeria*
[2]*Laboratory of Materials and Mechanics of Structure L.M.M.S,University of M'Sila, M'Sila, 28000, Algeria*
[3]*Laboratory of Water, Environment and Renewable Energies Laboratory, Med Boudiaf University, M'Sila, 28000, Algeria*

ARTICLE INFO

Article history
Received: 07 September 2024
Accepted: 10 December 2024

Keywords:
Andasol-1 Power Plant; Climatic Conditions; Parabolic Trough Concentrated Solar Power; M'Sila; Performance Assessment; SAM Software

ABSTRACT

Within the field of environmentally friendly electricity generation, parabolic trough concentrated solar power (CSP-PT) technology is acknowledged as one of the most efficient and practicable options. The current research employs the System Advisor Model (SAM) software to assess the viability of establishing a CSP facility utilizing parabolic trough technology, akin to the Andasol-1 power plant in southern Spain, within the M'Sila region of northern Algeria. It also statistically identifies the meteorological factors that most significantly influence Andasol-1's performance in M'Sila and models its operation based on them. Furthermore, it compares Andasol-1's performance across a range of locations reported in the literature. When the Andasol-1 power plant with a capacity of 50 MW is installed in M'Sila, it generates electricity year-round from 11:00 a.m. to 5:00 p.m., with an average output ranging from 25 MW_e to 52 MW_e. It can reach 17 hours of production, or even more, from March to September due to the favorable weather conditions and energy storage system (TES). The electricity generation increases with Direct Normal Irradiance (DNI) and ambient temperature, while it decreases with relative humidity. These variables collectively explain 98.2% of the electricity production variance in M'Sila ($R^2 = 0.982$), underscoring the significance of the linear regression model proposed. When Andasol-1 is erected in Kuwait, Tataouine (Tunisia), or at its true site (Spain), it produces less electricity annually than M'Sila, Tajoura (Libya), and Ma'an (Jordan). Furthermore, M'Sila's climate is the second most favorable for Andasol-1, after Jordan's, since it can generate 177.22 GWh of power annually there, exceeding its actual location. Climate change allows for the installation of solar power plants in northern regions as well.

Cite this article as: Bouchareb K, Ihaddadene N, Ihaddadene R, Belkhiri K. Comparative performance analysis of the Andasol-1 power plant in M'sila (an Algerian province. J Ther Eng 2025;11(5):1439−1454.

***Corresponding author.**
*E-mail address: nabila.ihaddadene@univ-msila.dz

This paper was recommended for publication in revised form by Editor-in-Chief Ahmet Selim Dalkiic

Published by Yıldız Technical University Press, İstanbul, Turkey
Yıldız Technical University. This is an open access article under the CC BY-NC license (http://creativecommons.org/licenses/by-nc/4.0/).

INTRODUCTION

In the environmentally friendly electricity generation area, concentrated solar power (CSP) technologies are recognized as one of the best and most practical alternatives [1]. Indeed, CSP technologies offer the advantage of incorporating a thermal energy storage system (TES), which may store excess heat energy generated during daytime overproduction for later usage when the sun is not shining [2], support grid stability, and secure dispatchability for on-demand electrical power, unlike other renewable energy technologies, such as wind power and photovoltaics [3].

The four CSP technologies that are currently on the market are the solar parabolic dish (SPD), linear Fresnel reflector (LFR), solar power tower, and parabolic trough collector (PTC) [4]. This latter technology is one of the most advanced and extensively used today. Indeed, when compared to other solar energy conversion technologies, the parabolic trough represents 76.6% of the overall market [5]. In addition, compared to solar towers and linear Fresnel technologies, parabolic trough technology is expected to maintain its dominance in the market [6,7,8,9]. Additionally, it has the ability to generate electricity either independently or in combination with conventional energy technologies at the lowest Levelized Cost of Electricity (LCOE) [10]. Moreover, parabolic trough collectors (PTCs) have also demonstrated their effectiveness in the field of water desalination [11,12].

Solar radiation is concentrated on an absorber tube in a parabolic trough collector (PTC) by large, curved mirrors in the shape of a U. Parabolic trough collectors are designed to track the sun along one axis, from east to west when they are aligned on the north-south axis, and from north to south when they are aligned on the east-west axis. Solar radiation heats a heat transfer fluid (HTF) running through the absorber tube, typically synthetic oil or water/steam. The thermal energy gathered in this way is transferred to a standard steam turbine power cycle to produce electricity.

With over 62 active projects, PTC is a well-established technology. Numerous theoretical studies have been published in the literature on the feasibility of integrating CSP based on parabolic collectors in various parts of the world. Following is a summary of some works on this subject.

Ismail A. et al. [13] investigated the feasibility of installing concentrated solar power (CSP) plants in Libya's capital (Tripoli) through an energetic, exergetic, and economic thermodynamic analysis. They found that installing the Andasol parabolic trough CSP plant in Tripoli provided a very positive return on investment, higher performance, and a decreased levelized cost of electricity (LCOE). Attai Y.A. et al. [14] compared a concentrated solar power plant to be installed in Aswan, South Egypt, to Palma del Rio II, a reference, to determine the relative benefit of constructing such a power plant in Aswan. The results obtained by the system advisor model (SAM) software show that Aswan produces electrical energy at a lower cost than Spain, and its annual CSP energy output is higher as well. Sultan A. J. et al. [15] evaluated the techno-economic performance of a parabolic trough solar power plant in Kuwait (desert climatic conditions and limited water supplies) and compared it to that of the reference plant in southern Spain (Andasol-1) for two design configurations employing wet and dry cooling options. The outcomes demonstrate that Kuwait outperformed Spain in terms of overall performance. Due to the DNI influence, ambient temperature, wind speed, and solar field heat loss/dumped energy, the Kuwait case performed better. Jilani N. A. et al. [16] conducted a techno-economic analysis of two CSP technologies—the parabolic trough collector (PTC) and the solar power tower (SPT)—in preparation for possible installation in Malaysia using two reference projects, the Andasol-1, and PS-10 systems in Spain, as references. The annual electricity generation and the initial cost are two critical aspects influencing the construction, installation, and deployment of PTC or SPT technology. Shagdar E. et al. [17] performed a numerical analysis both at nominal and part-load conditions of the 50 MW CSP's performance for four different reference days (i.e., March 22, June 22, September 22, and December 22), which correspond to the four seasons of the Mongolian climate. The findings indicate that solar radiation and solar incidence angle have a significant impact on the CSP plant's operating performance. The reference days outside of the winter constitute the best time with the highest operating performance for the 50 MW CSP plant. Additionally, the CSP plant's operating performance at part-load levels was noticeably lower than at nominal loads. Based on a reference plant design from Andasol-1 in southern Spain, Liqreina et al. [18] evaluated the competitiveness of dry cooling of steam power blocks of concentrating solar power (CSP) plants in comparison to wet cooling at the Ma'an site (desert zone) in southern Jordan. Although the cost of dry cooling is higher than that of wet cooling, dry cooled CSP plants are still a possibility in hot, arid areas with excellent solar resource, like Ma'an, and can even achieve lower costs than comparable wet-cooled plants situated in areas with less solar resource. Trabelsi et al. [19] investigated the influence of using molten salt as heat transfer fluid (HTF) in conjunction with dry cooling in a parabolic trough CSP plant at Tataouine, Tunisia, to significantly reduce the levelized cost of electricity (LCOE) and water use. In parabolic trough power plants, the results obtained indicate that molten salt is more economically advantageous than synthetic oil.

The feasibility of constructing solar power facilities in Algeria, like in many other countries, has been theoretically investigated, particularly in the country's desert region. Indeed, Achour et al. [20] investigated the performance of an Integrated Solar Combined Cycle (ISCC) plant under the southern Algerian climate through a developed thermodynamic model to assess solar radiation intensity as well as the overall performance of the hybrid solar power plant. It has been found that the amount of electricity produced increases with several operation parameters, such as the time of day, the mass flow rate of the heat transfer fluid, and the solar incidence angle on the collector surface. Benhaji et al. [21] performed a theoretical investigation using the System Advisor Model software (SAM) to evaluate and model a 100 MW parabolic trough-based solar thermal power plant with two different cooling systems: dry and evaporative condensers and thermal storage at Tamanrasset, southern Algeria. When comparing the power plant's electricity output to Tamanrasset's actual load demand, it was found that the plant will be able to supply 78% and 60% of the town's electrical demands throughout the winter and summer, respectively. Additionally, it was demonstrated that, compared to a normal electric generation system, the solar power plant may reduce carbon dioxide gas emissions by 2 million tons annually. With the aid of the System Advisor Model software, Ikhlef K. et al. [22] conducted a techno-economic evaluation of a 155 MW solar power plant (a 25 MW parabolic trough connected with a 130 MW gas turbine) known as the Solar Power Plant One (SPPI) located in Hassi R'mel (Algeria's southern region). They found that in the southern Algeria environment, wet cooling was more cost-effective than dry cooling and that Therminol VP1 was the optimal heat transfer fluid. Additionally, the best period for storage system optimization was four hours. Furthermore, integrating the backup system with the power plant increased annual energy output by 11.2% compared to the only solar field. Benabdellah H. M. et al. [23] carried out a techno-economic analysis of an Integrated Solar Combined Cycle (ISCC) power plant based on a Parabolic Trough Concentrator (PTC) system in Hassi R'mel (an Algerian Sahara region) with a new thermal storage system. They found considerable improvements in the efficiency of the power plant and the conversion of solar energy (up to 14%). The improved ISCC-PTC power plant at this location will enable savings of around 30 million dollars in natural gas consumption and 13 million dollars in emission taxes.

The current climate change (earth warming and water shortage) felt by earth's inhabitants (particularly since 2021) works in favor of increasing solar energy potential. Therefore, the exploitation of solar energy is not limited to desert areas; it can also be advantageous in northern regions. M'Sila, located in northern Algeria at the Sahara's gates, is a real example of the increase in its solar energy potential since 2008, according to the study done by Younes et al. [24]. Indeed, M'Sila, with global horizontal irradiation (GHI) of 1.79 MWh/m^2/year and direct normal irradiation (DNI) of 2117.93 kWh/m^2/year, is a suitable location for building concentrating solar power facilities [24]. This region deserves to be studied to see whether building a solar thermal power plant similar to that erected in Spain (Andasol-1) under its environment is feasible given its geographic location, which qualifies it to become an economic and development pole. Moreover, M'Sila's electricity usage has increased over the past ten years due to improved lifestyles [24]. Furthermore, government officials have paid close attention to encouraging investment in this area. For all these reasons, this study was carried out.

The originality of the current research lies in identifying the meteorological variables that have the most pronounced impact on the performance of Andasol-1 in M'Sila through stepwise linear regression and formulating a model for its electricity power generation based on these factors. Furthermore, the study compares Andasol-1's performance across various locations reported in the literature, rather than limiting the comparison solely to the reference location, Spain.

MATERIALS AND METHODS

The present theoretical investigation was conducted at M'Sila in northern Algeria to assess the performance of the reference power plant (Andasol-1), which has been operational since 2010 in southern Spain. The System Advisor Model (SAM) software, a commonly used tool to examine CSP plants, was utilized to perform this study. Meteorological data for the Andasol-1 site in Spain was supplied by the National Renewable Energy Laboratory via the SAM software library. Conversely, weather information for M'Sila was obtained from the METEONORM7 database. This meteorological data was input into the SAM software to simulate the performance of the CSP plant that will be erected by carrying out the following steps:

- Create a model base by simulating the reference solar power plant (Andasol-1), which has a capacity of 50 MW_e, at its actual site and comparing the findings with the real outputs.
- Simulate the reference plant under M'Sila's climatic conditions.
- Analyse the performance of the Andasol-1 solar power plant in M'Sila, with particular emphasis on the hourly annual energy distribution across the principal components of the solar installation, namely the solar field, the storage system, and the power block.
- Study of the effect of M'Sila's weather conditions on the Andasol-1's power output.
- Compare the performance of the Andasol-1 solar power plant with the different research projects carried out on the same plant in different countries, including its actual location in terms of net electricity generation, operating hours, SF efficiency, total plant efficiency, and water usage.

Technical Specifications Of The Reference Power Plant (Andasol-1)

The Andasol-1 plant, built by Solar Millennium, is the first parabolic trough plant in the world featuring a thermal storage technology [25]. It is close to Granada in southern Spain and had a 50 MWe maximum capacity when it first started operating in 2010 [26]. This plant covers 477 acres in total and primarily consists of a solar field, a thermal energy

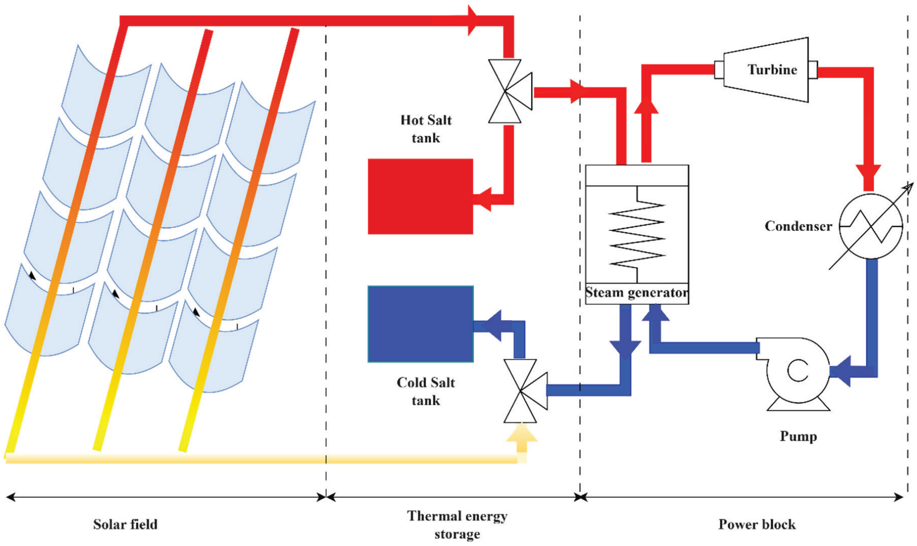

Figure 1. Schematic diagram of the Andasol-1 power plant.

storage system (TES), and a conventional power block. The solar collectors are arranged from north to south and rotate around this axis to follow the sun's daily course from east to west [27]. The main technical data for the reference plant is presented in Table 1 and was collected from published studies in the literature [15,25,26,28]. As depicted in Figure 1, the reference power plant primarily consists of a solar field, a thermal energy storage system (TES), and a conventional power block.

Table 1. Technical data of the reference plant (Andasol-1) [15,25,26,28]

Description	Value
Solar field	
Solar field aperture area	510,120 m^2
Number of loops	156
HTF type	Dowtherm A
Design loop inlet temperature	293°C
Design loop outlet temperature	393°C
Collector	
Collector type EuroTrough	ET150
Length of one single collector	148.5 m
Aperture width of a collector	5.77 m
Focal length	1.71 m
Row spacing	17.3 m
Mirror reflectivity	93.5%
Optical efficiency	75%
Total collectors	624
Reflective aperture area	817.5 m^2
Storage system	
Full load storage hours	7.5 h
Storage fluid	Molten salt
Thermal storage capacity	1085.53 MWh_{th}
Cold tank temperature	292°C
Hot tank temperature	386°C
Power Block	
Nominal capacity	50 MW_e
Turbine inlet pressure	100 bar
Rated cycle conversion efficiency	38%
Cooling system type	Wet

Description of the Selected Site

As previously mentioned, the M'Sila location was chosen for this study to evaluate the Andasol-1 solar power plant's performance in the M'Sila environment.

Given its distinctive geographic location, the province of M'Sila is regarded as one of the most prominent provinces in Algeria's highlands. M'Sila, a town in northern Algeria with 1,387,158 residents and an area of 18,175 km^2, lies about 250 kilometers south of Algiers, the country's capital [29].

According to geographic coordinates, it is located at 4° 32’43” longitude, 35° 42’07” latitude, and 441 m altitude. More than half of M’Sila’s lands have a slope of less than 3%. In that province, the industry sector comes in first with a share of 57.86%, followed by the construction materials sector in second place with a share of 19.54%, and the service sector in third place with a share of 16.34% [30]. An 880-MW power plant is also present there [29].

Meteorological Data for the Selected Site

Concentrated solar power plants’ performance and efficiency are significantly influenced by the local weather where they are installed. For M’Sila (the chosen site), the SAM software needs meteorological data such as direct normal irradiation (DNI) and ambient temperature to

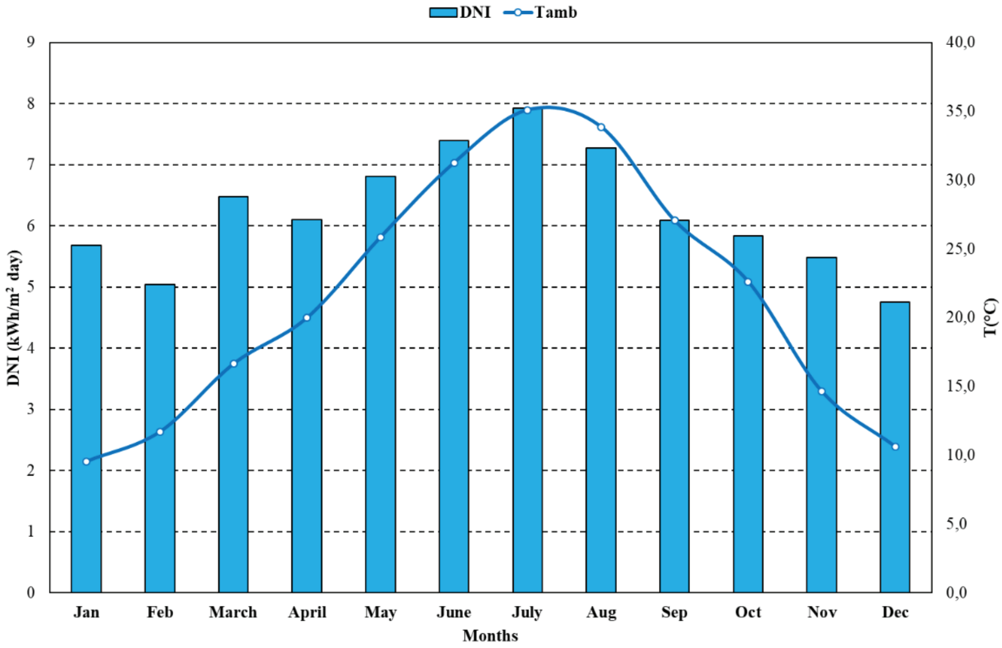

Figure 2. Monthly average daily direct normal irradiation and temperature in M'Sila.

perform the current investigation. Since it represents the average of all the years for which measurements are available, the METEONORM7 database generates meteorological data for one year, regarded as a typical year [21]. A Typical Meteorological Year file (TMY3) was downloaded from this software database, which includes hourly measurements of several meteorological parameters.

Figure 2 shows the monthly average daily direct normal irradiation and the monthly average daily temperature in M'Sila. It can be observed that, aside from February and December, the monthly average daily direct normal irradiation (DNI) value for the M'Sila location exceeds 5.5 kWh/ m^2/day all year long. Moreover, the smallest DNI value of 4.75 kWh/m2/day was recorded in December, while the maximum DNI value of 7.93 kWh/m2/day was registered in July. Further, it is estimated that M'Sila receives 2282.54 kWh/m2/year of direct normal irradiation (DNI) annually. The majority of the current CSP plants are erected in sites where the DNI value does not surpass 2153.5 kWh/ m2/year [31]; hence, M'Sila is qualified to have CSP plants installed because of its significant DNI. It should be noted that M'Sila is today classified as an arid region [24] with low precipitation, especially over the past two years, as a result of the climate change it has undergone.

One of the fundamental meteorological parameters that exerts a significant impact on the heat dissipation of various CSP plant configurations is the ambient temperature. In M'Sila, a predominant range of hourly temperatures fluctuates between 10 and 32 °C. The issue concerning the potential freezing of the heat transfer fluid Therminol VP-1 emerges during the winter season in M'Sila due to the possibility of temperatures dropping below 12 °C (Figure 2).

Furthermore, January recorded the lowest average monthly temperature at 9.5 °C, while July experienced the highest average monthly temperature at 35 °C (Figure 2).

The winds in M'Sila vary from calm winds to moderate breezes. In that region, the wind speed can thus change from 0 m/s to 4.8 m/s. Furthermore, only April sees wind speeds greater than 4 m/s; for the remainder of the year, the wind blows at less than 4 m/s.

CSP-PT PLANT'S ENERGY ANALYSIS

Assuming steady-state operating conditions, the energy analysis based on thermodynamic laws is carried out as follows for each component of a CSP-PT power plant:

The incident annual radiative solar power ($P_{sun,incident}$) on the solar field's net aperture area (A_{ap}) is given as [15]:

$$P_{sun,\ incident} = \sum_{i=1}^{365} \sum_{j=0}^{23} DNI_{ij} A_{ap} \tag{1}$$

The following formula provides the net aperture area of the solar field [15]:

$$A_{ap} = W_{ap}\ L\ M\ N = \sum_{i=1}^{N_{SCA}} A_{collector,i} \tag{2}$$

Where W_{ap} is the width aperture of the collector shown in Figure 3, L is the length of the collector, M is the number of collector rows in series (see Figure 1), N is the number of parallel lines (see again Figure 1), and N_{SCA} is the entire number of collectors in the solar field.

DNI_{ij} is the direct normal irradiance incident on the net aperture area of the solar field during the hour j of the day i.

The radiation incident on the solar field's net aperture area is greater than that incident on the absorber tube due to optical losses, which minimize the PTC's heat uptake from direct incident irradiation. These two quantities are connected by the optical efficiency ($h_{optical}$) of the collector, given as follows:

$$\eta_{optical} = \frac{P_{absorber}}{P_{sun,\, incident}} \tag{3}$$

Where $P_{absorber}$ is the annual power received on the absorber tube.

The heat flux absorbed by the heat transfer fluid (HTF) is represented by the thermal power output from the parabolic trough collector (Q_u), which also accounts for the heat power incident on the absorber tube and that lost from it into the environment [15,26], as depicted in Figure 3. It is given by:

$$Q_u = R_1 R_2\ A_{ap} N \left[F_R(\tau\alpha)_n IAM\, I_{beam} - \frac{F_R U_L}{ConcRat}(T_{in}\text{-}T_{amb}) \right] \tag{4}$$

In which,

$$R_1 = \frac{M\,\dot{m}\,Cp_{fluid}}{A_{ap}} \left(\frac{1\text{-}e^{((\text{-}F'\ U_L\ A_{ap})/(M\,\dot{m}\,Cp_{fluid}))}}{R_{test}} \right) \tag{5}$$

$$R_{test} = g_{test} Cp_{fluid} \left(1\text{-}e^{(\text{-}F'\ U_L/(g_{test} Cp_{fluid}))} \right) \tag{6}$$

$$F'\ U_L = \begin{cases} F_R\ U_L & si \dfrac{F_R\ U_L}{g_{test}\, Cp_{fluid}\, ConcRat} \geq 1 \\ g_{test}\, Cp_{fluid} \left(1\text{-}e^{\left(\frac{F_R\ U_L}{g_{test}\, Cp_{fluid}\, ConcRat}\right)} \right) & si \dfrac{F_R\ U_L}{g_{test}\, Cp_{fluid}\, ConcRat} \prec 1 \end{cases} \tag{7}$$

$$ConcRat = \frac{A_{ap}}{A_{absorber}} \tag{8}$$

$$R_2 = \frac{1\text{-}\left(1\text{-}((R_1\ A_{ap} F_R U_L)/(\dot{m}\ Cp_{fluid} M\ ConcRat))\right)^M}{M\left((R_1\ A_{ap} F_R U_L)/(\dot{m}\ Cp_{fluid} M\ ConcRat)\right)} \tag{9}$$

Where $F_R(\tau\alpha)_n$ represents the efficiency when the solar radiation is absorbed by the absorber tube and removed by the HTF, $F'U_L$ is the modified loss coefficient, IAM is the incidence angle modifier, I_{beam} is the amount of the beam solar radiation incident on the collector surface, T_{in} is the temperature of the HTF entering the collector array, T_{amb} is the ambient temperature, ConcRat is the concentration ratio between the aperture area and the absorber area, and is the mass flow rate of the HTF.

From the above, the absorber thermal efficiency ($h_{thermal}$) can be defined as the ratio of power acquired by the HTF to that incident on the absorber tube. The formula below provides it:

$$\eta_{thermal} = \frac{P_{HTF}}{P_{absorber}} = 1\text{-}\frac{P_{th,loss}}{P_{sun,incident}\ \eta_{optical}} \tag{10}$$

Similarly, the solar field efficiency (h_{SF}) shown below can be identified as the ratio of the power acquired by the HTF to the incident power on the net aperture area of the solar field:

$$\eta_{SF} = \frac{p_{HTF}}{P_{sun,incident}} \tag{11}$$

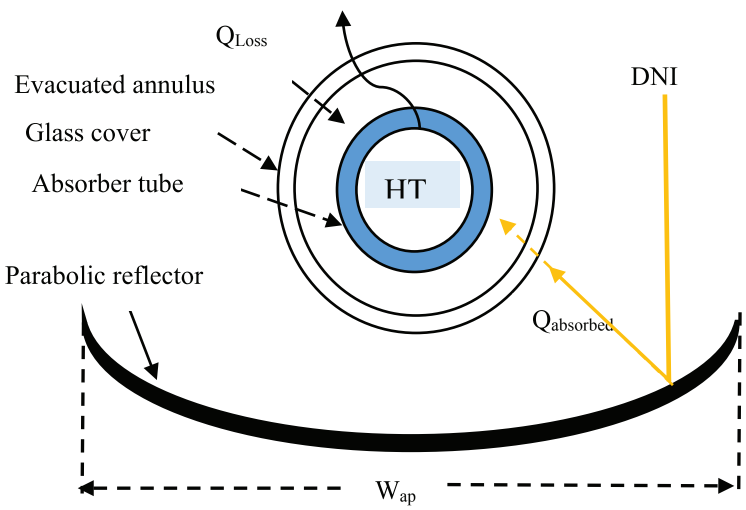

Figure 3. Parabolic trough collector's heat exchanges.

It should be noted that this annual efficiency can also be evaluated on an hourly, daily, and monthly basis.

The amount of DNI that is prevented from reaching the collector by mirror defocusing is known as the dumped energy or total defocused thermal energy resulting from the solar field (SF). The discarded power (Q_{dump}) is provided as [15,26]:

$$Q_{dump}=A_{ap}\ DNI\ \eta_{optical}\ \eta_{def}=\dot{m}\ Cp_{fluid}(T_{out}-T_{max}) \quad (12)$$

Where T_{max} is the highest temperature at which the fluid may leave the collector, h_{def} is the ratio of defocused SCA units, and Tout is the temperature of the fluid at the collector outlet, given as [15,26]:

$$T_{out}=\begin{cases} T_{in}+\dfrac{Q_u}{\dot{m}\ Cp_{fluid}} & si\ \dot{m}\succ 0 \\ T_{amb}+F_R(\tau\alpha)_n IAM\ I_{beam}\dfrac{ConcRat}{F_R\ U_L} & si\ \dot{m}=0 \end{cases} \quad (13)$$

The dumped energy can be simulated by SAM software on an hourly basis.

Considering the heat exchanger's thermal losses, the net power block efficiency ($\eta_{net,PB}$) shows how well thermal input is converted to electric output. It's presented as:

$$\eta_{net,PB}=\frac{P_{elc,turb}-P_{ele,pompe}-P_{aux,cond}}{(P_{HTF}-P_{loss,piping})}=\frac{P_{ele,net,PB}}{(P_{HTF}-P_{loss,piping})} \quad (14)$$

Where $P_{ele,turb}$ is the electric power output of the steam turbine in MW; $P_{ele,pump}$ is the consumption rate of the condensate and feed water pumps; $P_{aux,cond}$ is the consumption rate of the condenser auxiliary; $P_{loss,piping}$ is the thermal losses rate in the piping; and $P_{ele,net,PB}$ is the power block's net power output in MW.

The ratio of the electric power generated by the solar power plant to the solar power incident on the solar field is the overall solar to electric efficiency of the plant ($\eta_{overall}$), which is determined along with the other efficiencies as follows:

$$\eta_{overall}=\eta_{optical}\eta_{thermal}\eta_{piping}\eta_{net,PB}\eta_{aux,SF}=\frac{P_{ele,a}}{P_{sun,incident}} \quad (15)$$

$P_{ele,a}$ is the steam turbine's annual electric power output measured in MW; $\eta_{aux,SF}$ is the SF auxiliary's efficiency, expressing the effect of the SF tracking consumptions and circulating pumps on the net PB output; and η_{piping} is the piping efficiency, assessing the effect of thermal losses in the piping, including those that occur at night, on the heat transfer fluid (HTF) used to transfer thermal power.

The thermal energy storage capacity of the TES system, measured in hours of thermal energy delivered at the thermal input level of the power block design, is known as the full load hours of the TES. It is calculated as follows [15,32]:

$$Q_m^{TES}=N_h^{TES}\frac{P_{elec,PB}}{\eta_{PB}} \quad (16)$$

Where Q_m^{TES} is the thermal energy storage capacity of the TES system, N_h^{TES} is the number of full load hours of storage, and $P_{elec,\ PB}$ is the power block's power output.

RESULTS AND DISCUSSION

Results Validation

This section's aim is to compare the SAM simulation results for the Andasol-1 reference plant, located in southern Spain, with the real and simulated outputs published by Herrmann et al. [28], Bataineh et al. [33], and Sultan et al. [15] in order to show the accuracy of the simulation process. There are reasonable deviations, as demonstrated by Table 2, which displays our simulation results along with real and simulated data for the Andasol-1 power plant published in the literature. The percentage discrepancies for the performance of the Spanish reference power plant between the

Table 2. Outcomes on the operation of the Andasol-1 power plant under its location's climate conditions, both real and simulated

Description	Unit	Published data (Herrmann et al. [28])	Published data (Bataineh et al. [33])	Published data	Our simulation (Sultan et al [15])
Annual DNI	kWh/m^2	2202	2052	2033.3	2034.7
Annual solar irradiation on the SF	MWh/a	1,105,430	—	1,037,586.6	1,037,932
Annual thermal power from the SF	MWh/a	510,030	—	479,609.8	473,996.5
Annual net electricity output	MWh_e/a	157,206	153,560.0	151,569.8	151.282.5
Annual solar field efficiency	%	46.1	44.2	46.2	45.7
Annual overall efficiency	%	14.7	13.1	14.6	14. 6
Number of full load hours of steam Turbine	h	3144	3098	3003	3056
Total water consumption	m^3/a	612,000.00	—	508,949.0	584,541.0

Table 3. Percentage differences between the reported results related to the reference power plant's performance under its location's climate

Description	(% difference)					
	Bataineh et al.[33]. compared to	Sultan et al.[15]. compared to		Simulated data from this work compared to		
	Herrmann et al. [28]	Herrmann et al. [28],	Bataineh et al. [33]	Herrmann et al. [28],	Bataineh et al. [33],	Sultan et al. [15]
Annual DNI	-7.31	-8.30	-0.92	-8.22	-0.85	0.07
Annual Solar irradiation on the solar field	—	-6.54	—	-6.5	—	0.03
Thermal power from the solar field	—	-6.34	—	-7.6	—	-1.18
Annual net electricity output	-2.37	-3.72	-1.31	-3.92	-1.51	-0.19
Annual overall efficiency	-12.21	-0.68	10.27	-0.69	10.27	0.0
Annual solar field efficiency	-4.29	0.22	4.33	-0.88	3.28	-1.1
Number of full load hours of steam Turbine	-1.48	-4.70	-3.16	-2.8	-1.35	1.76
Total water consumption	—	-20.25	—	-4.7	—	12.93

simulated results taken into consideration (mentioned in Table 2) and the actual data are displayed in Table 3. Our simulation, as can be seen, approaches that of Sultan et al. [15], which, on the whole, is not too far from the real data reported by Hermann et al. [28], particularly in terms of yearly overall plant efficiency, yearly net electricity output, thermal power from the solar field, and annual solar field efficiency.

Indeed, for all investigated parameters, the difference between our simulation findings and the actual operating results of the Andasol-1 central is less than 9%. Since SAM simulation software can accurately predict the actual data of the reference plant, it will be utilized in the following sections to assess its performance in the M'Sila climate and compare it to the Andasol-1 reference plant in Spain and, on the other hand, to the simulated works of the same plant in different parts of the world.

Andasol-1 Power Plant Simulation Under M'sila Climate Conditions

The following part discusses how power varies throughout the various components of the simulated Andasol-1 power plant when it is operating in M'Sila.

The hourly annual distribution of the thermal power generated by the solar field is shown in Figure 4. As can

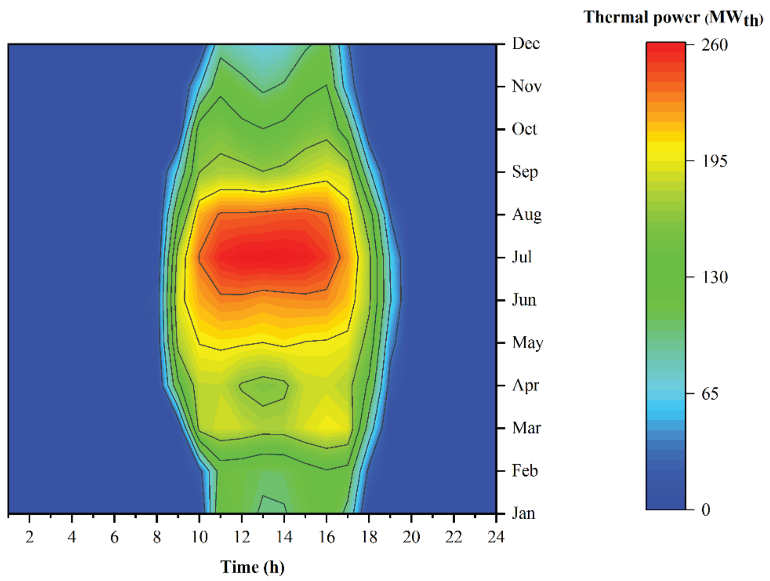

Figure 4. Hourly annual distribution of the thermal power generated by the solar field of Andasol-1 under the climatic conditions of M'Sila.

be observed, the hourly solar field's thermal power production peak occurs during the summer months (from June to August), with values ranging from 230 to 267 MW_{th}/hour. However, this peak is at its lowest during the winter months. Indeed, it doesn't go above 150 MW_{th}/hour. Furthermore, the spring and autumn seasons record values between 135 MW_{th}/hour and 204 MW_{th}/hour for the hourly solar field's thermal power output peak. Moreover, the Andasol-1 solar field, when installed in M'Sila, generates thermal power from 11:00 a.m. to 5:00 p.m. throughout the year, ranging between 77.70 MW_{th} and 256 MW_{th} on average. In May, June, and July, thermal energy production can last up to 12 hours, starting at 8 a.m. and ending at 7 p.m.

The thermal power production of the Andasol-1 solar field situated in M'Sila varies over the course of the year. Specifically, this solar power plant demonstrates its highest thermal power output during the summer months and its lowest during the winter season, with average capacities of 2292 MW_{th} and 728 MW_{th}, respectively. Moreover, the average thermal power production during spring surpasses that of autumn, with mean values standing at 1746 MW_{th} and 1178 MW_{th}, respectively.

Figure 5 shows the power available in the thermal storage system (TES) of the proposed solar power plant in M'Sila over the year on an hourly basis. It is evident that, given its direct correlation with DNI level, the TES system is inefficient in the winter and crucial in the summer, with average values of 57 and 703 MW_{th}, respectively. Moreover, the maximum hourly thermal power in the thermal storage system, which ranges from 86 to 123 MW_{th}/hour, is evidently noticed to occur in the summer (June to August).

Nevertheless, in the winter months, this peak is at its lowest since it doesn't exceed 25 MW_{th}/hour. In addition, the hourly storage system's thermal power peak is recorded at 21 MW_{th}/hour to 70 MW_{th}/hour in the spring and autumn. Further, when erected in M'Sila, the Andasol-1 power plant's storage system stores thermal power year-round from 11:00 a.m. to 4:00 p.m., ranging between 3 MW_{th} and 102 MW_{th} on average. The TES system accumulates thermal power from 9:00 a.m. to 5:00 p.m. from April through September, or even until 6:00 p.m. in May and June.

The hourly annual distribution of electrical power generated by the proposed solar power plant in M'Sila, which is the final electrical power ready to be delivered to the grid, is depicted in Figure 6. As seen, the Andasol-1 power plant, when located in M'Sila, produces the most electricity during the summer and the least during the winter, with average values of 745 and 235 MW_e, respectively. Moreover, the average electrical power output in the spring is higher than that in the fall, averaging 562 and 389 MW_e, respectively. It is clear that the summer months of June through August are when the hourly power production peak, which averages 52 MW_e/hour, occurs. Still, this peak is at its lowest during the winter because it never rises above 40 MW_e/hour. Furthermore, in the spring and fall, the hourly electricity production peak ranges from 41 MW_e/hour to 48 MW_e/hour. Further, when the Andasol-1 power plant is installed in M'Sila, it generates electricity year-round from 11:00 a.m. to 5:00 p.m., with an average output ranging from 25 MW_e to 52 MW_e. It can reach 17 hours of production, or even more, from March to September due to the favorable weather conditions and energy storage system (TES), as seen above.

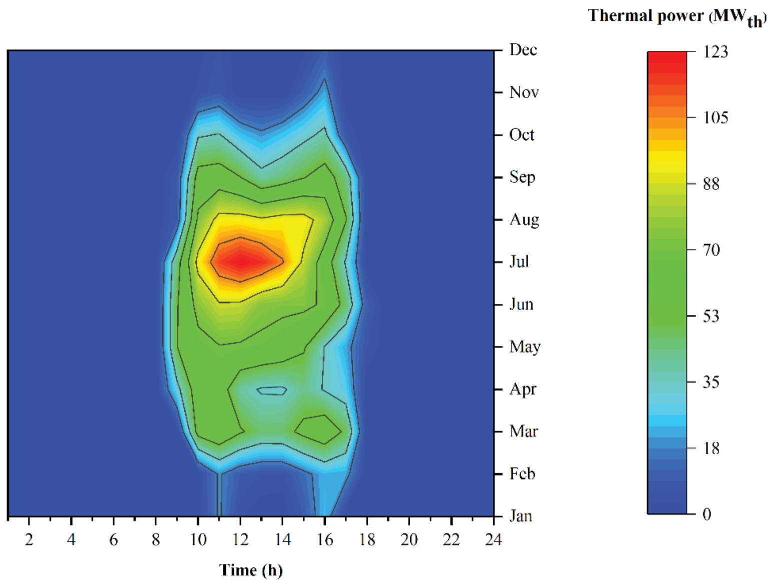

Figure 5. Hourly annual distribution of the thermal power accumulated by the TES of Andasol-1 under the climatic conditions of M'Sila.

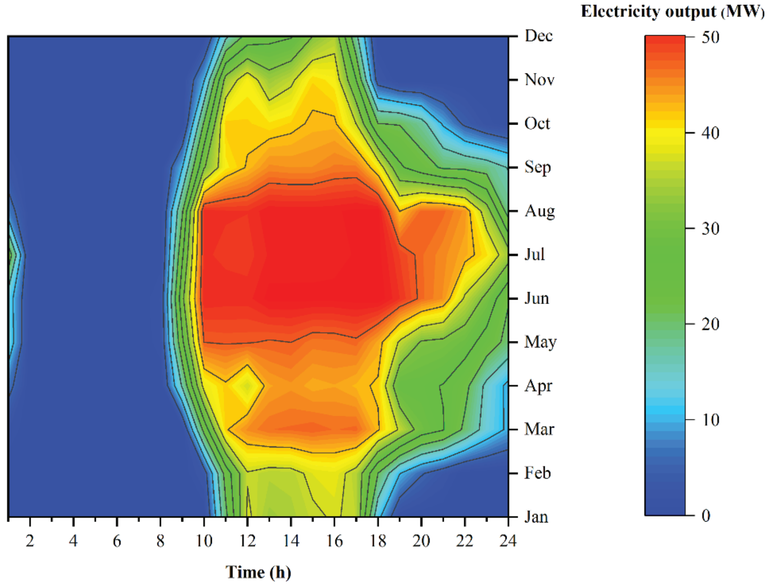

Figure 6. Hourly annual distribution of the electricity output by the Andasol-1 under the climatic conditions of M'Sila.

Figure 7 displays the proposed CSP-PT power plant's monthly net electricity production in conjunction with the meteorological conditions in M'Sila. As seen, the Andasol-1 power plant in M'Sila generates 24.15 GWh of electrical energy at its maximum in July and 4.81 GWh at its minimum in December. These values correspond to M'Sila's monthly maximum and minimum recorded DNI, respectively. Moreover, as the ambient temperature rises, so does the net electrical output, and vice versa. Further, relative humidity and net electricity production are inversely related. The lowest relative humidity practically coincides with the maximum productivity, and vice versa. However, the net electricity output is not impacted by the wind since it blows at less than 4 m/s most of the time in M'Sila, except for April (the windiest month), where the production records a slight decrease.

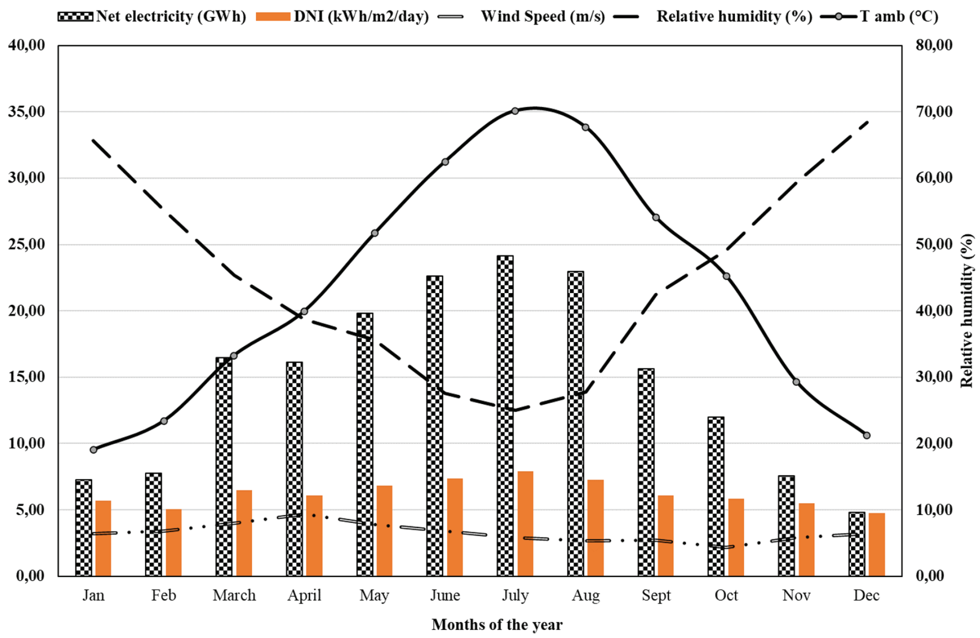

Figure 7. Andasol-1 power plant's monthly net electricity production in conjunction with the meteorological conditions in M'Sila.

Our results are in agreement with those reported in the literature [15,26,34] regarding the effect of DNI and ambient temperature on the functioning of Andasol-1 (net electricity production) in different regions of the world. Furthermore, in contrast to the existing qualitative studies cited above, we suggest using stepwise linear regression—a quantitative study—to identify the meteorological factors that have the most significant effect on M'Sila's clean electricity output. The findings of stepwise linear regression on the impact of weather conditions on Andasol-1's power output, when sited in M'Sila, are displayed in Table 4.

As seen, DNI, temperature, and relative humidity are significant factors affecting electricity production in M'Sila since their p-values are less than 0.05 (significant level). Furthermore, this statistical analysis reaffirms that, when situated in M'Sila, wind speed has no discernible impact on the power plant's production.

When combined, the variables DNI, temperature, and relative humidity account for 98.2% of the variance in electricity production in M'Sila (R^2=0.982 in Table 4). In this regard, we propose the following model, which describes the power generation in M'Sila based on the most influential hourly weather conditions:

$$P = 287.03 + 0.009 \times DNI - 5.482 \times T - 3.342 \times phi \quad (17)$$

Where,

P is the net power output in MW, DNI is the direct normal irradiance in W/m^2, T is the dry temperature in °C, and phi is the relative humidity in %.

Additionally, Table 4 (ANOVA) indicates that the suggested model is significant with F(3,20) = 361.583 and P (significance F)<0.05.

The PCA (Principal Component Analysis) approach is another statistical study performed to evaluate the contribution of the months of the year in the production of power in M'Sila. The outcomes indicate that 86.42% of the variance in the hourly annual production is accounted for by the seven months of July, June, August, May, April, September, and March; the remaining months, December, January, November, February, and October, account for 11.26% of the variance. Stated differently, the generation of electricity throughout the summer, spring, and the first month of autumn accounts for 78% of the total yearly output, surpassing 15 GWh/month. Production stays below 12 GWh per month in the winter and the remaining autumn months.

Andasol-1 Power Plant Simulation Under Different Climate Conditions

The simulated net electricity generated by Andasol-1 is shown in Figure 8 on a monthly and annual basis in different regions, each with its own environmental parameters. Andasol-1, which generates 189.05 GWh of power yearly in Jordan's Ma'an, a cold desert region, has demonstrated its ability to function efficiently in these conditions. The second climatic condition favorable to Andasol-1 is that of M'Sila (arid climate, according to our recent work [24]), where it can produce 177.22 GWh of electricity annually. Furthermore, the subtropical desert steppe climate of Tajoura, Libya, enables Andasol-1 to achieve nearly the same amount of electricity annually as M'Sila. When Andasol-1 is erected in Kuwait, Tataouine, Tunisia, or at its true site (Spain), it produces less electricity annually than M'Sila, Tajoura, and Ma'an. A difference of more than 11 GWh can be noticed. Once more, the site's environment has a significant impact on the CSP power plant's net output production.

Table 4. Effect of meteorological conditions on Andasol-1's power output using stepwise linear regression

Regression Statistics					
Multiple R		0.991			
R Square		**0.982**			
Adjusted R Square		0.979			
Standard Error		2.632			
Observations		24			
ANOVA					
	df	***SS***	***MS***	***F***	***Significance F***
Regression	3	7512.461	2504.154	361.583	**0.000**
Residual	20	138.511	6.926		
Total	23	7650.971			
		Coefficients	***Standard Error***	***t Stat***	***P-value***
Intercept		287.0336794	95.20558914	3.014882656	**0.00684**
Hourly Data: **Resource Beam normal irradiance (W/m^2)**		0.008920514	0.003467863	2.572337228	**0.01818**
Hourly Data: **Resource Dry bulb temperature (°C)**		-5.481630697	2.510739957	-2.183272976	**0.04110**
Hourly Data: **Relative humidity (%)**		-3.341774233	0.901347004	-3.707533523	**0.00139**

J Ther Eng, Vol. 11, No. 5, pp. 1439−1454, September, 2025

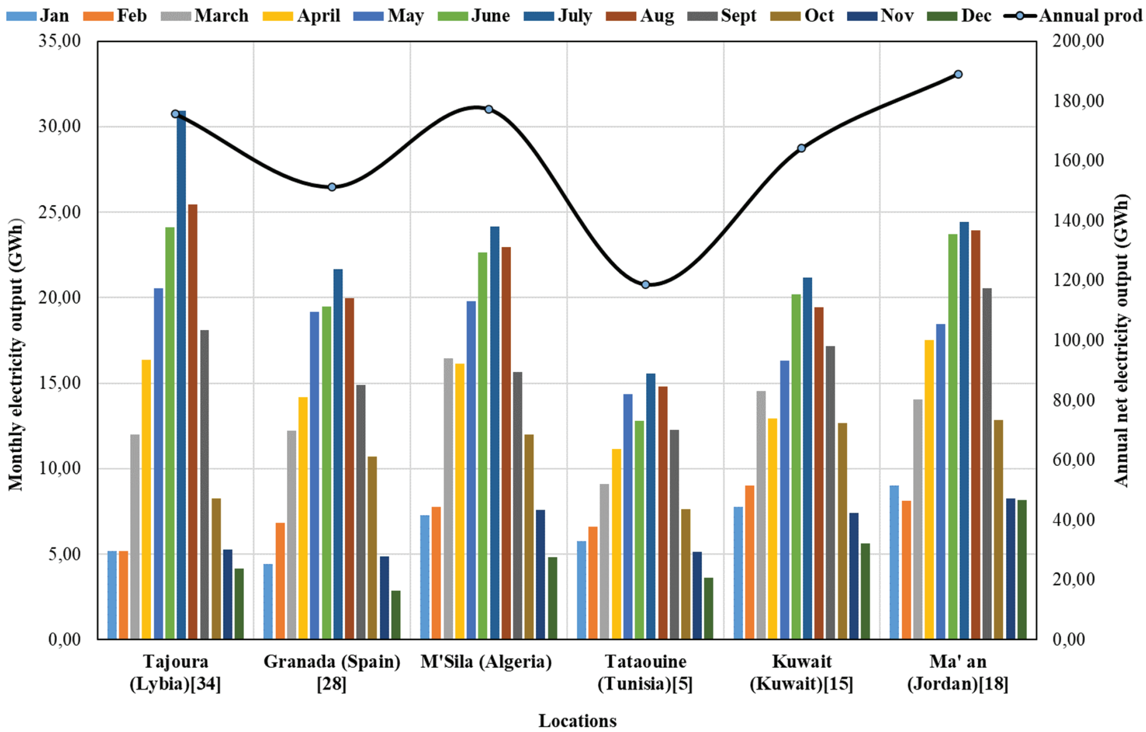

Figure 8. Andasol-1 power plant's monthly and annual net electricity production in different zones in the world.

Regardless of where in the northern hemisphere it is located, Andasol-1 produces the most power in July and the least in December; nevertheless, the extreme values reached differ from place to place (Figure 8). As it appears, Andasol-1, situated in Tajoura, Libya, can produce up to 30.93 GWh of electricity in July, compared to 15.56 GWh in Tataouine, Tunisia, over the same period. Moreover, when located in Ma'an, Jordan, it may produce up to 8.14 GWh of electricity in December, compared to 2.87 GWh at its actual location in Spain.

Andasol-1 generates more electricity at all of the locations under consideration during the summer, spring, and first month of fall. More than 74% of the yearly production is produced during this time. During the winter and the remaining autumn months, the net electrical energy produced remains below 13 GWh/month, except in Tataouine, where it falls below 8 GWh/month. Further, Andasol-1, constructed in M'Sila, generates more electricity monthly than it does in its current location all year round.

As seen in Figures 8 and 9, of all the regions examined, Ma'an (Jordan) has the highest annual DNI (2693 kWh/

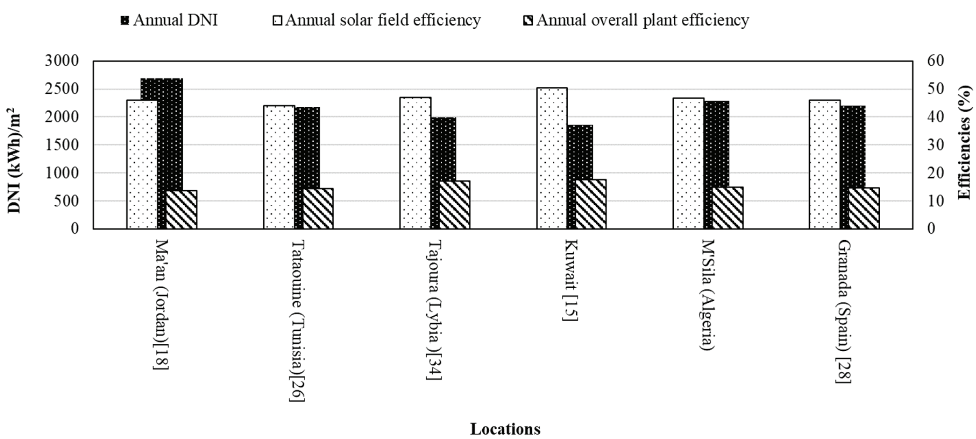

Figure 9. DNI of the zones studied and efficiencies of the Andasol-1 installed there.

m^2) [18], producing, thus, the maximum amount of clean electricity. Conversely, Kuwait, with the lowest annual DNI (1857.1 kWh/m^2) [15], produces more electricity than southern Spain because of its highest ambient temperature and lowest wind speed, which result in the highest solar field efficiency of 50.3% (lowest heat loss from the solar field). Furthermore, Tataouine in Tunisia has the lowest solar field yield of the sites under investigation, at 44.02% [5]. Kuwait has the greatest annual overall plant efficiency, with an annual efficiency of 17.5%, while Ma'an in Jordan has the lowest efficiency, at 13.8%. Southern Spain and M'Sila exhibit nearly identical overall efficiency.

The highest number of operating hours at full load (4399 h) of Andasol-1 is seen at Ma'an, whose DNI is the highest [18]. M'Sila, Kuwait, and Southern Spain (the actual site) follow with 3580 h, 3306 h [15], and 3144 h [28] of full load running, respectively. Moreover, Andasol-1 offers the lowest running hours at full load (2548 h) in Tataouine, Tunisia [5].

Again, Andasol-1, erected in Ma'an, consumes the highest amount of water, 751617.7 m^3/year [18], instead of 592799 m^3/year (the least amount) when installed in Kuwait [15]. Andasol-1 in M'Sila uses more water than Spain, Tataouine, and Kuwait, with values of 674301 m^3/year, 612000 m^3/year [28], 649735 m^3/year [26], and 592799 m^3/year [15], respectively.

Under the climatic circumstances of M'Sila, the discarded power (Q_{dump}) is estimated to be 8046.86 MW/year. It is recorded, as in southern Spain, during the period from March to September, with July having the highest value.

From the above, it is clear that the location affects the solar thermal power plant's performance significantly. Moreover, it is better to discuss the combined impact of the site's meteorological variables (DNI, temperature, relative humidity, and wind speed) rather than each one separately.

CONCLUSION

The increasing global demand for energy and the negative environmental impacts associated with traditional energy sources have made the transition to renewable energy sources imperative. In this context, the present theoretical study aims to assess the feasibility of implementing Andasol-1, an operational solar thermal power plant located in Spain, within M'Sila, a desert region in Algeria, utilizing SAM software. Meteorological data for M'Sila were obtained from the METEONORM7 database and served as input for the SAM software.

The following results are to be retained:

- When installed in M'Sila, the Andasol-1 solar power plant is projected to generate thermal power averaging between 77.70 MWth and 256 MWth from 11:00 a.m. to 5:00 p.m. throughout the year. It will store thermal power from 11:00 a.m. to 4:00 p.m., with an average range of 3 MWth to 102 MWth annually. The facility will produce electricity from 11:00 a.m. to 5:00 p.m., yielding an average output of 25 MWe to 52 MWe year-round.
- The meteorological factors that most significantly influence clean electricity generation in M'Sila are direct normal irradiance (DNI), temperature, and relative humidity, which collectively account for 98.2% of the variance in electricity production ($R^2 = 0.982$). The climate of M'Sila ranks as the second most favorable for Andasol-1 after Jordan's climate since it can produce an annual total of 177.22 GWh of electricity—surpassing its current operational site.
- Furthermore, by deploying concentrated solar power (CSP) units utilizing parabolic trough technology, M'Sila can alleviate pressure on its thermal power plant during summer months while simultaneously reducing greenhouse gas emissions.

NOMENCLATURE

Acronyms

CSP	Concentrated solar power
CSP-PT	Parabolic trough concentrated solar power
GHI	Global horizontal irradiation
HTF	Heat transfer fluid
IEA	The International Energy Agency
ISCC	Integrated Solar Combined Cycle
LCOE	Levelized cost of electricity
LFR	Linear Fresnel reflector
NREL	National Renewable Energy Laboratory ()
PCA	Principal Component Analysis
PTC	Parabolic trough collector
PV	Photovoltaic
Q_{inc}	Incident solar energy on the solar field per unit time
Q_{field}	Thermal energy produced by the solar field per unit time
Q_{inp}	Thermal energy that enters the power block per unit time
Q_{st}	Change in the amount of thermal energy in the storage system per unit time
SAM	System Advisor Model
SF	Solar field
SCA	Solar Collector Assembly
SNL	Sandia National Laboratories
SPPI	Solar Power Plant One
SPD	Solar parabolic dish
SPT	Solar power tower
TES	Thermal energy storage
TMY3	Typical Meteorological Year file
W_{net}	Net electrical power produced by the solar power plant

Symbols

A_{ap}	Solar field's net aperture area (m^2)
ConcRat	Concentration ratio between the aperture area and the absorber area (–)

DNI	Direct normal irradiation (W/m^2)
F’	Collector efficiency factor (-)
FR	Collector heat removal factor (-)
$F_R(\tau\alpha)_n$	The efficiency when the solar radiation is absorbed by the absorber tube and removed by the fluid (–)
IAM	Incidence angle modifier (–)
I_{beam}	Amount of beam solar radiation incident on the collector surface (W/m^2)
L	Collector length (m)
M	Number of rows of collectors in series (–)
$\dot{m}$	Mass flow rate of fluid (kg/h)
N	Number of parallel lines (–)
N_{SCA}	Total number of collectors (–)
N_h^{TES}	Number of full load hours of storage (–)
P	Net power output in MW
$P_{sun,incident}$	Radiative solar power incident on net aperture area (MW)
$P_{absorber}$	Annual power received on the absorber tube (MW)
$P_{aux,cond}$	Condenser auxiliaries consumption rate (MW)
$P_{ele,turb}$	Steam turbine electric power output (MWe)
$P_{ele,pump}$	Condensate and feedwater pump consumption rate (MW)
$P_{loss,piping}$	Piping thermal losses rate(MW)
$P_{ele,net,PB}$	Net power output from the power block (MW)
$P_{elec,\ PB}$	Power block’s power output (MW)
$P_{th,SF}$	Thermal power delivered by the solar field at the design point (MW)
$P_{th,in,PB}$	Power block’s thermal power need at nominal conditions (MW)
$P_{ele,a}$	Annual net electricity output (MW)
Phi	Relative humidity (%)
Q_u	Thermal power output from the solar field (MW)
Q_m^{TES}	Thermal energy storage capacity (MWh)
Q_{dump}	Dumped thermal power from the solar field (MW)
T	Dry temperature in (°C)
T_{amb}	Ambient temperature (°C)
T_{in}	Temperature of the HTF entering the collector array (°C)
T_{max}	Highest temperature at which the fluid may leave the collector (°C)
T_{out}	Temperature of the fluid at the collector outlet (°C)
U_L	Loss coeffcient (W/m^2°C)
W_{ap}	Width aperture of the collector (m)

Greek symbols

$h_{thermal}$	Thermal effciency (%)
h_{SF}	Solar field efficiency (%)
$h_{optical}$	Optical efficiency (%)
$\eta_{net,PB}$	Net power block effciency (%)
$\eta_{overall}$	Annual overall plant effciency (%)
$\eta_{aux,SF}$	Effciency of solar feld auxiliary (%)
η_{piping}	Piping effciency (%)

AUTHORSHIP CONTRIBUTIONS

Authors equally contributed to this work.

DATA AVAILABILITY STATEMENT

The authors confirm that the data that supports the findings of this study are available within the article. Raw data that support the finding of this study are available from the corresponding author, upon reasonable request.

CONFLICT OF INTEREST

The author declared no potential conflicts of interest with respect to the research, authorship, and/or publication of this article.

ETHICS

There are no ethical issues with the publication of this manuscript.

STATEMENT ON THE USE OF ARTIFICIAL INTELLIGENCE

Artificial intelligence was not used in the preparation of the article.

REFERENCES

[1] Khan J, Arsalan MH. Solar power technologies for sustainable electricity generation - A review. Renew Sustain Energy Rev 2016;55:414–425. [CrossRef]

[2] Awan AB, Zubair M, Chandra Mouli KVV. Design, optimization and performance comparison of solar tower and photovoltaic power plants. Energy 2020;199:117450. [CrossRef]

[3] Dinter F, Gonzalez DM. Operability, reliability and economic benefits of CSP with thermal energy storage: First year of operation of ANDASOL 3. Energy Procedia 2014;49:2472–2481. [CrossRef]

[4] Islam MT, Huda N, Abdullah AB, Saidur R. A comprehensive review of state-of-the-art concentrating solar power (CSP) technologies: Current status and research trends. Renew Sustain Energy Rev 2018;91:987–1018. [CrossRef]

[5] Balghouthi M, Trabelsi SE, Ben Amara M, Ali ABH, Guizani A. Potential of concentrating solar power (CSP) technology in Tunisia and the possibility of interconnection with Europe. Renew Sustain Energy Rev 2016;56:1227–1248. [CrossRef]

[6] Pavlović TM, Radonjić IS, Milosavljević DD, Pantić LS. A review of concentrating solar power plants in the world and their potential use in Serbia. Renew Sustain Energy Rev 2012;16:3891–3902. [CrossRef]

[7] Suresh NS, Thirumalai NC, Rao BS, Ramaswamy MA. Methodology for sizing the solar field for parabolic trough technology with thermal storage and hybridization. Sol Energy 2014;110:247–259. [CrossRef]

[8] Ouagued M, Khellaf A, Loukarfi L. Estimation of the temperature, heat gain and heat loss by solar parabolic trough collector under Algerian climate using different thermal oils. Energy Convers Manag 2013;75:191–201. [CrossRef]

[9] Yılmaz İH, Mwesigye A. Modeling, simulation and performance analysis of parabolic trough solar collectors: A comprehensive review. Appl Energy 2018;225:135–174. [CrossRef]

[10] Baharoon DA, Rahman HA, Omar WZW, Fadhl SO. Historical development of concentrating solar power technologies to generate clean electricity efficiently – A review. Renew Sustain Energy Rev 2015;41:996–1027. [CrossRef]

[11] Kedar S, Bewoor A, Murali G, More GV, Roy A. Thermal analysis of sea water hybrid solar desalination system - an experimental approach. Int J Heat Technol 2024;42:1349–1358. [CrossRef]

[12] Kedar S, Murali G, Bewoor AK. Mathematical modelling and analysis of hybrid solar desalination system using evacuated tube collector (ETC) and compound parabolic concentrator (CPC). Math Model Eng Probl 2021;8:45–51. [CrossRef]

[13] Ehtiwesh IAS, Neto Da Silva F, Sousa ACM. Deployment of parabolic trough concentrated solar power plants in North Africa – a case study for Libya. Int J Green Energy 2019;16:72–85. [CrossRef]

[14] Attai YA, Megallaa KF, Aziz SS. Comparison for performance of concentrated parabolic trough power plant in Egypt & Spain. Int J Emerg Technol Adv Eng 2015;5:327-333.

[15] Sultan AJ, Hughes KJ, Ingham DB, Ma L, Pourkashanian M. Techno-economic competitiveness of 50 MW concentrating solar power plants for electricity generation under Kuwait climatic conditions. Renew Sustain Energy Rev 2020;134:110342. [CrossRef]

[16] Jailani NA, Ahmad A, Norazahar N. A techno-economic analysis of parabolic trough collector (PTC) and solar power tower (SPT) as solar energy in Malaysia. J Energy Saf Technol 2021;4:13–28. [CrossRef]

[17] Shagdar E, Lougou BG, Sereeter B, Shuai Y, Mustafa A, Ganbold E, Han D. Performance analysis of the 50 MW concentrating solar power plant under various operation conditions. Energies 2022;15:1–24. [CrossRef]

[18] Liqreina A, Qoaider L. Dry cooling of concentrating solar power (CSP) plants, an economic competitive option for the desert regions of the MENA region. Sol Energy 2014;103:417–424. [CrossRef]

[19] Trabelsi SE, Qoaider L, Guizani A. Investigation of using molten salt as heat transfer fluid for dry cooled solar parabolic trough power plants under desert conditions. Energy Convers Manag 2018;156:253–263. [CrossRef]

[20] Achour L, Bouharkat M, Behar O. Performance assessment of an integrated solar combined cycle in the southern of Algeria. Energy Reports 2018;4:207–217. [CrossRef]

[21] Benhadji Serradj DE, Sebitosi AB, Fadlallah SO. Design and performance analysis of a parabolic trough power plant under the climatological conditions of Tamanrasset, Algeria. Int J Environ Sci Technol (Tehran) 2022;19:3359-3376. [CrossRef]

[22] Ikhlef K, Larbi S. Techno-economic optimization for implantation of parabolic trough power plant: Case study of Algeria. J Renew Sustain Energy 2020;12:063704. [CrossRef]

[23] Benabdellah HM, Ghenaiet A. Energy, exergy, and economic analysis of an integrated solar combined cycle power plant. Eng Reports 2021;3:1–25. [CrossRef]

[24] Kherbiche Y, Ihaddadene N, Ihaddadene R, Hadji F, Mohamed J, Beghidja AH. Solar energy potential evaluation. Case of study: M'Sila, an Algerian province. Int J Sustain Dev Plan 2021;16:1501–1508. [CrossRef]

[25] National Renewable Energy Laboratory. System Advisor Model (SAM) Case Study. pp. 1–10. Available at: https://sam.nrel.gov/images/web_page_files/sam_case_csp_physical_trough_andasol-1_2013-1-15.pdf Accessed on Sep 05, 2025.

[26] Trabelsi SE, Chargui R, Qoaider L, Liqreina A, Guizani A. Techno-economic performance of concentrating solar power plants under the climatic conditions of the southern region of Tunisia. Energy Convers Manag 2016;119:203–214. [CrossRef]

[27] Andasol 1 project. Available at: https://solarpaces.nrel.gov/project/andasol-1 Accessed on January 20, 2023.

[28] Herrmann U, Geyer M. The AndaSol Project. Workshop on thermal storage for trough power systems 2002; February 20–22.

[29] Monograph on the Province of M'Sila, National Agency for Intermediation and Land Regulation (ANIREF), Ministry of Industry. Available at: https://www.aniref.dz/DocumentsPDF/monographies/MONOGRAPHIE%20WILAYA%20MSILA.pdf Accessed on April 6, 2023.

[30] http://dim-msila.dz/?p=267 Accessed on April 6, 2023.

[31] Abbas M, Merzouk NK, Belgroun Z, Aburidah H. Parametric study of the installation of a solar power tower plant under Saharan climate of Algeria: Case study of Tamanrasset. In: Proceedings of the First International Conference on Nano-electronics, Communications and Renewable Energy (ICNCRE 2013) 2013:357–362.

[32] Blair N, Dobos A, Freeman J, Neises T, Wagne M, Ferguson T, Gilman P, Janzou S. System Advisor Model, SAM 2014.1.14, General Description. NREL Report No. TP-6A20-61019; National Renewable Energy Laboratory (NREL): Golden, CO, USA, 2014; p. 19. [CrossRef]

[33] Bataineh KM, Gharaibeh A. Optimization analyses of parabolic trough (CSP) plants for the desert regions of the Middle East and North Africa (MENA). Jordan J Mech Ind Eng 2018;12:33–43.

[34] Belgasim B, Aldali Y, Abdunnabi MJR, Hashem G, Hossin K. The potential of concentrating solar power (CSP) for electricity generation in Libya. Renew Sustain Energy Rev 2018;90:1–15. [CrossRef]